Available online at www.sciencedirect.com
ScienceDirect
Journal of Photochemistry and Photobiology A: Chemistry 194 (2008) 105–109
Journal of Photochemistry and Photobiology A:Chemistry
www.elsevier.com/locate/jphotochem

Excited-state proton transfer and geminate recombination in the molecular cage of β-cyclodextrin

Young-Shin Lee, Oh-Hoon Kwon [1], Han Jung Park, Jan Franz [2], Du-Jeon Jang *

School of Chemistry, Seoul National University, NS60, Seoul 151-742, Republic of Korea

Received 5 April 2007; received in revised form 9 July 2007; accepted 25 July 2007
Available online 31 July 2007

Abstract

Excited-state proton transfer and geminate recombination in aqueous heptakis(2,6-di-*O*-methyl)-β-cyclodextrin have been compared with those in water by monitoring the photoinduced prototropic tautomerization of 6-hydroxyquinoline, which occurs via forming anionic intermediate. Enol deprotonation decelerates by 18 times whereas its reverse process accelerates slightly with encapsulation. The imine protonation of the intermediate slows down by 8.2 times in the molecular cage. These unusual kinetic features have been explained with the geminate recombination of protons as well as the structural dynamics of solvent molecules and the relative energetics of involved species.

Keywords: Excited-state proton transfer; Heptakis(2,6-di-*O*-methyl)-β-cyclodextrin; 6-Hydroxyquinoline; Geminate recombination; Solvation energy

1. Introduction

Proton transfer attracts considerable attention because it plays a key role in a wide variety of biological and chemical phenomena [1–8]. The dynamics of proton transfer is determined by the size, the structure, and the motion of a solvent cluster as well as by the nature of a prototropic group [5,8–10], whereas the rate of proton migration is controlled by solvent structural dynamics [6–8,10]. Hydroxyquinolines and their derivatives having two prototropic groups in a molecule have been extensively explored [7,9–18]. The enolic and the imino groups of 3-, 6-, and 7-hydroxyquinoline become much more acidic and basic, respectively, in S_1 than in S_0 [7,9–12,15]. Thus, their normal species (HOQN) undergoes the excited-state tautomerization of enol deprotonation and imine protonation stepwise in water via forming anionic intermediate species ($^-$OQN) [10,14,15]. However, the tautomeric form ($^-$OQNH$^+$) of 6-hydroxyquinoline (6HQ) has been reported to have a quinonoidal structure at S_1 [14,16]. Cyclodextrins, attracting interests in the field of artificial catalysts, consist of α, D-glucose subunits and possess nonpolar cavities with polar rims containing primary hydroxyl and secondary methoxy groups [19–22]. A number of studies have reported the effects of micelles and cyclodextrins on proton transfer to shed light on the influence of lipophilic environment [18–26].

7-Hydroxyquinoline is reported to undergo excited-state proton transfer (ESPT) in the molecular cage of aqueous β-cyclodextrin [17,18]. The anionic intermediate during ESPT forms slower but decays faster in β-cyclodextrin cages than in water [18]. However, the fluorescence spectral overlaps of HOQN, $^-$OQN, and $^-$OQNH$^+$, as well as the low solubility (in water) and the low association constant (with 7-hydroxyquinoilne) of β-cyclodextrin, make the ESPT kinetics of 7-hydroxyquinoline very complex. Furthermore, both processes of enol deprotonation and imine protonation occur too rapidly for us to investigate their reverse processes in detail. These have led us to investigate the ESPT of 6HQ in the molecular cage of heptakis(2,6-di-*O*-methyl)-β-cyclodextrin (CD). CD is a derivative of β-cyclodextrin with a greatly improved solubility in water, encapsulating 6HQ with a large association constant [26]. In this letter, we demonstrate that the dynamics of ESPT

* Corresponding author. Fax: +82 2 889 1568.
E-mail address: djjang@snu.ac.kr (D.-J. Jang).
[1] Present address: Laboratory for Molecular Sciences, California Institute of Technology, Pasadena, CA 91125, USA.
[2] Present address: Department of Physics and Astronomy, University College London, London WCIE 6BT, UK.

1010-6030/$ – see front matter © 2007 Elsevier B.V. All rights reserved.
doi:10.1016/j.jphotochem.2007.07.021

can be effectively modulated by enclosing 6HQ in CD to change the geminate recombination of protons as well as the structural dynamics of solvent molecules and the relative energetics of involved species.

2. Experimental

6HQ purchased from Sigma–Aldrich was further purified via column chromatography, while CD and ^2H_2O (isotopic purity ≥ 99.9%) were used as received from Sigma–Aldrich. Aqueous 6^{1}HQ or 6^{2}HQ was prepared by dissolving 6HQ in triply distilled water or in ^2H_2O, respectively. p^{1}H and p^{2}H were adjusted by adding aqueous ^{1}HCl or NaO^{1}H and ^{2}HCl or NaO^{2}H, respectively. The p^{2}H was corrected from the pH meter reading [27]. Results presented here were obtained at pH 7 and at room temperature.

Absorption spectra were obtained by employing a spectrometer (Scinco, S-3100), while fluorescence spectra were measured with excitation at 315 nm by using a home-built fluorometer. Fluorescence kinetic profiles were detected with a 10 ps streak camera (Hamamatsu, C2830) by exciting samples at 315 nm with pulses from a Raman shifter pumped by a Nd:YAG laser of 30 ps (Quantel, YG 701). Relative solvation energies were calculated using a self-consistent field method with a polarizable continuum model. The geometry was optimized at S_1 with a time-dependent density functional theory using the BP86 (Becke exchange and Perdew correlation) functional and the TZVP (triple ζ valence polarized) basis set [28].

3. Results and discussion

Fig. 1a shows that the lowest $^1(\pi, \pi^*)$ absorption band of HOQN in water shifts to the red with the addition of CD. However, one expects that $^1(\pi, \pi^*)$ absorption shifts to the blue in CD because polarity in CD is smaller than that in water. Thus, we consider that decrease in hydrogen bonding with encapsulation shifts to the red in CD [20,29]. One can also argue that decrease in hydrogen bonding should shift $^1(\pi, \pi^*)$ absorption to the blue instead. The drastic increase of HOQN acidity with excitation is suggested to bring the red absorption shift in CD. Nonetheless, this spectral change suggests that 6HQ in water incorporates into the hydrophobic interior of CD and that the dipole moment of HOQN at S_1 is greater than that of HOQN at S_0 because of increase in enol acidity and imine basicity with excitation (vide infra). It is recently reported [26] that 6HQ enters the molecular cages of CD in water with the association constant of 295 M^{-1} to form a 1:1 6HQ-CD complex having its imino group inside the cage and its enolic group at the wider rim of the CD cage (Scheme 1). Thus, we suggest that at least 97% of 6HQ molecules in our samples having 6HQ of 0.1 mM and CD of 128 mM are encapsulated in CD molecular cages.

The excitation of HOQN in bare water gives a fluorescence spectrum consisting of three distinctive bands emitted from HOQN at 387 nm, $^-$OQN at 462 nm, and $^-$OQNH$^+$ at 568 nm (Fig. 1b) [10]. This indicates that ESPT is operative within the lifetime of HOQN. With the gradual addition of CD, fluorescence from HOQN and $^-$OQN shifts to the blue whereas that

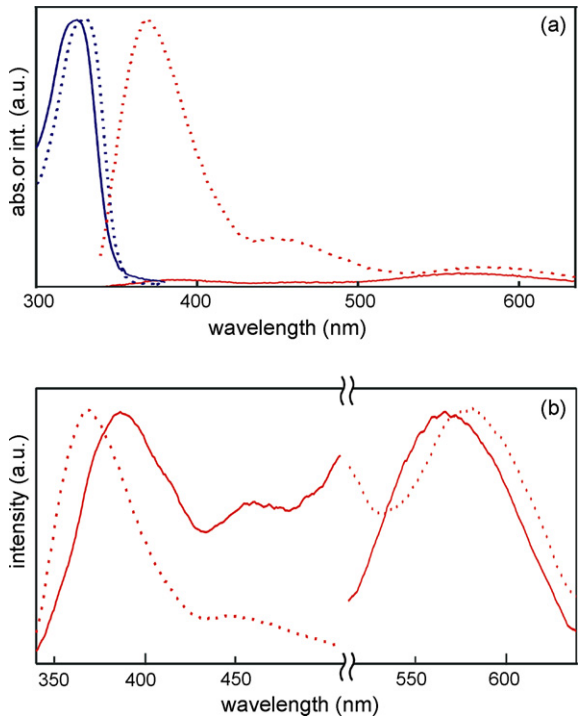

Fig. 1. Absorption (blue) and fluorescence spectra (red) (a) and maximum-normalized fluorescence spectra (b) of 0.1 mM 6HQ in water having 0 (solid) and 128 mM CD (dotted). The left and the right sides of the *x*-axis break in b are separately normalized.

from $^-$OQNH$^+$ shifts to the red. The same $^1(\pi, \pi^*)$ transition of HOQN displays a large bathochromic solvatochromism in absorption but a significant hypsochromic one in emission. This indicates that the dipole moment of HOQN increases greatly with excitation [30]. The increase of the dipole moment results from the drastic increase of both enol acidity and imine basicity with excitation [11,18]. Whereas $^-$OQNH$^+$ at S_0 has zwit-

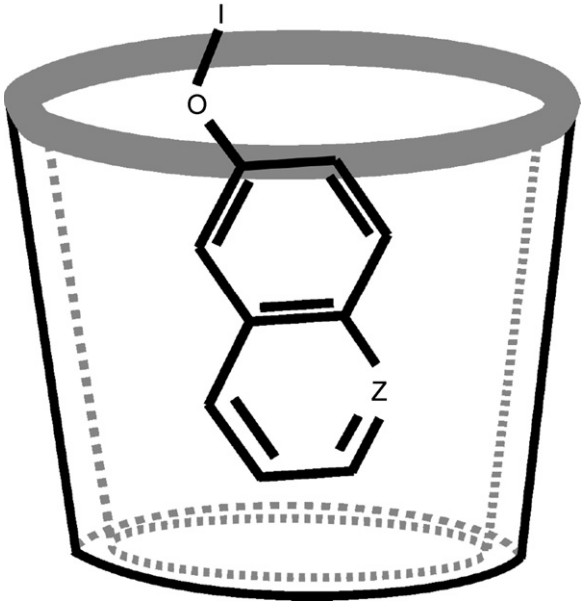

Scheme 1. Schematic for the inclusion complex of 6HQ with CD.

terionic character with a large charge separation, that at S_1 possesses more quinonoidal character. Thus, the dipole moment of the tautomeric species of 6HQ is much smaller at the excited state than that at the ground state [13]. Although $^{-}$OQNH^{+} having quinonoidal character is more stable at S_1, $^{-}$OQNH^{+} having zwitterionic character becomes more unstable at S_0 in the hydrophobic interior of CD than in water, resulting in the red shift of $^{-}$OQNH^{+} fluorescence in the cages [18]. This suggests that the electronic structures of 6HQ prototropic species are modified energetically in the cavities to show different ESPT dynamics from that free in water (vide infra). While the encapsulation of 6HQ in CD enhances $^{-}$OQNH^{+} fluorescence by 50%, it raises HOQN fluorescence enormously by a factor of 40. This suggests that CD encapsulation can be utilized to enhance the luminescence of fluorophosphorescent molecules.

The excitation of HOQN gives three distinctive fluorescence kinetic profiles of HOQN, $^{-}$OQN, and $^{-}$OQNH^{+} (Fig. 2). It has been already reported that the tautomerization of HOQN occurs consecutively to produce $^{-}$OQNH^{+} via forming $^{-}$OQN as the intermediate species [10]. The fluorescence kinetic profiles of CD-encapsulated 6HQ are remarkably slower than those of CD-free 6HQ, indicating that tautomerization and relaxation processes are slowed down in CD molecular cages. Kinetic constants extracted from the exponential rise and decay fits of Fig. 2 are given in Table 1. Although the fluorescence of each prototropic species was monitored without being interfered with by the emission of the other two species, the fluorescence kinetic constants of HOQN and $^{-}$OQN are very similar each other. This designates that the reverse processes of 6HQ tautomerization should be considered as well to fit the fluorescence kinetic profiles of 6HQ. We consider that the extensive contribution of the reverse processes in CD makes the kinetic constants in Table 1 more complicated than those in water. The proton-transfer and relaxation processes of excited 6HQ prototropic species can be depicted as shown in Scheme 2, where k_N, k_A, and k_T denote the radiative and nonradiative relaxation rate constants of HOQN, $^{-}$OQN, and $^{-}$OQNH^{+}, respectively.

Following the global analysis of Giestas et al. [31], we have conducted the numerical analysis of extracted kinetic constants in Table 1 to obtain the rate constants of Scheme 2. The mechanism of Scheme 2 translates into the differential equation:

$$\frac{\mathrm{d}}{\mathrm{d}t}\begin{bmatrix}\mathrm{HOQN}\\ {}^{-}\mathrm{OQN}\\ {}^{-}\mathrm{OQNH}^{+}\end{bmatrix} = \begin{bmatrix}-X & k_{-1} & 0\\ k_2 & -Y & k_{-2}\\ 0 & k_2 & -Z\end{bmatrix} \times \begin{bmatrix}\mathrm{HOQN}\\ {}^{-}\mathrm{OQN}\\ {}^{-}\mathrm{OQNH}^{+}\end{bmatrix} \quad (1)$$

where $X = k_1 + k_N$, $Y = k_{-1} + k_2 + k_A$, and $Z = k_{-2} + k_T$. The literature values of $2.5 \times 10^8\ s^{-1}$ and $5.8 \times 10^7\ s^{-1}$ have been employed for k_N and k_A, respectively [32].

Table 2 indicates that encapsulation in CD molecular cages retards both the enol deprotonation of HOQN and the imine protonation of $^{-}$OQN enormously. However, the reverse process of HOQN deprotonation in CD becomes slightly faster than that in water or the forward process in CD. Because ionic $^{-}$OQN is inferred to be more unstable in cages due to the hydrophobic environment than in water, encapsulation makes the deprotonation of HOQN to form $^{-}$OQN energetically unfavorable. Thus,

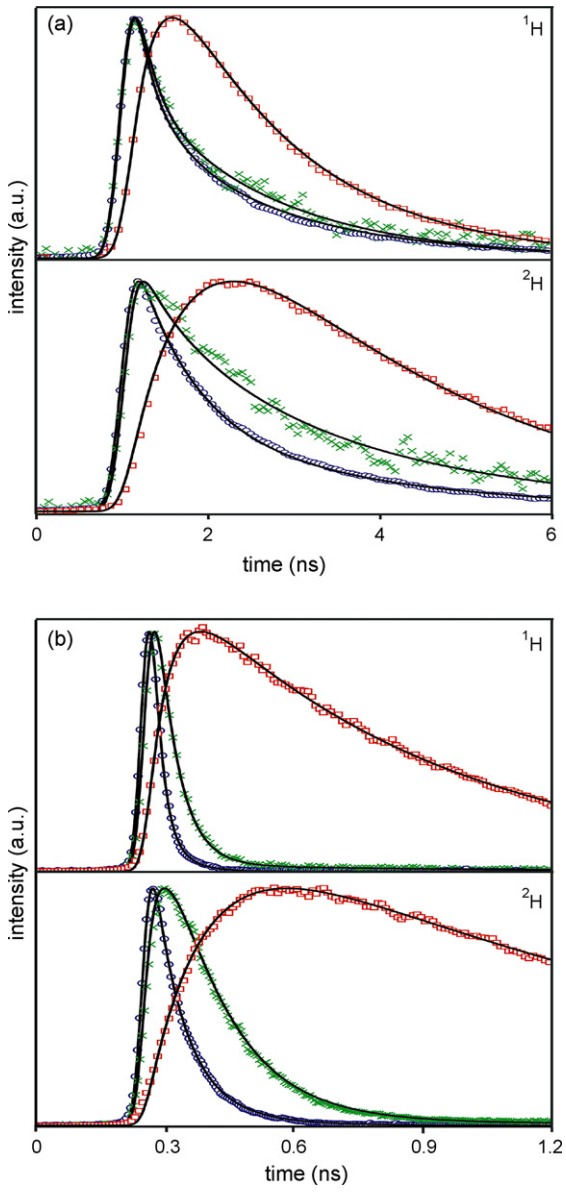

Fig. 2. Emission kinetic profiles of 0.1 mM 6HQ with (a) and without 128 mM CD (b) in ^1H_2O (^{1}H) and ^2H_2O (^{2}H) and their best fitted curves (lines), excited at 315 nm and monitored at 360 (blue), 470 (green) and 610 nm (red).

the retardation of enol-deprotonation is thought to result mainly from the altered acid–base energetics of 6HQ in CD. The kinetic isotope effect (KIE) of HOQN deprotonation decreases by 1.7 times whereas that of $^{-}$OQN protonation to form $^{-}$OQNH^{+} decreases by 2.5 times with encapsulation. The large changes of KIEs with encapsulation are also considered to originate from the unfavorable energetics of 6HQ and the slowed rate of solvent relaxation in hydrophobic molecular CD cages as well. Unfavorable energetics and slow solvent relaxation for the formation of

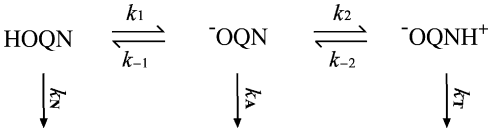

Scheme 2. ESPT and relaxation processes of excited 6HQ prototropic species.

Table 1
Isotope-dependent kinetic constants of 6HQ fluorescence in water with and without CD

Isotope[a]	[CD] (mM)	λ_{em} (nm)	Time constant[b] (ps)
^{1}H	0	380	19 (0.854)[c] + 48 (0.146)
		480	19 (−0.280) + 48 (0.980) + 617 (0.020)
		600	48 (−1.000) + 617 (1.000)
^{1}H	128	380	130 (0.350) + 425 (0.330) + 1500 (0.320)
		480	130 (−0..235) + 425 (0.762) + 1500 (0.238)
		600	130 (−0.360) + 425 (−0.640) + 1500 (1.000)
^{2}H	0	380	67 (0.865) + 130 (0.135)
		480	67 (−0.595) + 130 (0.998) + 1332 (0.002)
		600	130 (−1.000) + 1332 (1.000)
^{2}H	128	380	184 (0.232) + 846 (0.555) + 2550 (0.213)
		480	184 (−0.531) + 846 (0.724) + 2550 (0.276)
		600	184 (−0.064) + 846 (−0.936) + 2550 (1.000)

[a] Isotope of protic hydrogen.
[b] Estimated experimental errors at [CD] = 0 are in the range of 2–5 ps while those at [CD] = 128 mM are in the range of 7–18 ps.
[c] Negative and positive values of initial relative amplitudes indicate rise and decay time constants, respectively.

Table 2
Tautomerization and relaxation rate constants and their KIEs[a] of CD-encaged 6HQ[b] in water

Isotope[c]	k_1 ($\times 10^9$ s^{-1})	k_{-1} ($\times 10^9$ s^{-1})	k_2 ($\times 10^9$ s^{-1})	k_{-2} ($\times 10^9$ s^{-1})	k_T ($\times 10^9$ s^{-1})
^{1}H	2.6 (48)	2.9 (2.6)	2.8 (23)	0.88[d]	1.3 (1.6)
^{2}H	1.3 (14)	1.9 (0.45)	2.6 (8.2)	0.39[d]	0.50 (0.75)
	2.0 (3.4)	1.5 (5.8)	1.1 (2.8)	2.3[e]	2.6 (2.1)

[a] Given in the third row.
[b] Values of CD-free 6HQ are shown in parentheses.
[c] Isotope of protic hydrogen.
[d] Too small compared with other rate constants.
[e] Not available.

an ionic species by encapsulation in the hydrophobic interior are suggested to decrease the contribution of the tunneling process in its ESPT. Encapsulation in the hydrophobic interior removes the barrier of $^-$OQN protonation to form $^-$OQNH$^+$. The activation-controlled reaction of protonation to the imino group of $^-$OQN in water becomes almost solvent-controlled in CD.

The roles of water clusters as proton acceptors are rather not important for the deprotonation of strongly photoacidic HOQN [18]. Thus, the retardation of enol deprotonation in CD can be attributed to the altered acid–base energetics of 6HQ prototropic species as well as the slow solvation of water encapsulated 6HQ. The reduced rate constant of HOQN deprotonation in CD is in accordance with the picture of a free-energy relationship to the rate constant of an activated ESPT process [33,34]. Energetic modification is considered to be also operative in the imine protonation of $^-$OQN. The formation of a water cluster to donate a proton is essential for the imine protonation of $^-$OQN because the quinoline moiety of 6HQ is surrounded by the hydrophobic interior of CD. Furthermore, the KIE value of $^-$OQN protonation falls off from 2.8 to 1.1 by inclusion in CD. This suggests a mechanistic switch of the activation-controlled protonation process into a solvation-controlled one. Therefore, the acceleration of imine protonation by energetic alteration in the hydrophobic cages seems to be superimposed by deceleration in the structural dynamics of water molecules to form proton-donating water clusters.

The solvation energies of prototropic species involved in the tautomerization of excited 6HQ have been calculated to understand the influence of solvation on ESPT dynamics (Table 3). The change of the solvent from bulk water having a dielectric constant of 78 to a cavity-confined water having a dielectric constant of 40 increases the energies of all involved species. The effect is the largest on $^-$OQN due to its charge as discussed. The computational result that $^-$OQN is more unstable than HOQN agrees with the experimental result that k_1 becomes much smaller in CD cavities than in bulk water. Cavities reduce solvent polarity and increase cage effects, enhancing the geminate recombination of protons substantially [20,21]. Because the enolic group of 6HQ is exposed to the surroundings of bulk

Table 3
Calculated solvation energies ($\Delta_{sol}G^\circ$) of 6HQ prototropic species at S_1

Species	$\Delta_{sol}G^\circ$ (kJ mol^{-1})		$\Delta(\Delta_{sol}G^\circ)$[a] (kJ mol^{-1})
	Free[b]	Encaged[c]	
HOQN	−26.3	−25.1	+1.2
$^-$OQN	−210.1	−206.5	+3.6
$^-$OQNH	−72.5	−70.3	+2.2

[a] $\Delta_{sol}G^\circ$ (encaged) − $\Delta_{sol}G^\circ$ (free).
[b] Calculated at ε_r of 78, the relative permittivity of bulk water [35].
[c] Calculated at ε_r of 40, the estimated relative permittivity of water confined in CD [36].

water, the deprotonation of HOQN occurs near the rim of CD. The formation of a water cluster to accept a proton seems to be important as well in the rate-determining step of enol deprotonation. The polysugar torus surrounding the enolic group disturbs the hydrogen bond in the intermediate vicinity of the proton and the enolate group produced during enol deprotonation. This, together with the instability of the charged anionic intermediate, enhances the geminate recombination of the proton to yield the remarkably large value of k_{-1}. We suggest that the migration of the proton produced during enol deprotonation to the imino group to form $^{-}$OQNH^{+} [10,15] also competes with the geminate recombination.

In summary, we have observed kinetic changes in the proton transfer and relaxation of prototropic species involved in the excited-state tautomerization of aqueous 6HQ with encapsulation in CD. HOQN undergoes tautomerization to produce $^{-}$OQNH^{+} stepwise via forming an intermediate species of $^{-}$OQN, as reported in CD-free water. Enol deprotonation decelerates by 18 times whereas its reverse process accelerates slightly with encapsulation. The imine protonation of the intermediate in CD also becomes slower by 8.2 times than that in water. The extensively decelerated proton dissociation and accelerated reverse reaction of the enolic group are due to the geminate recombination of the proton and the instability of the charged anion in the hydrophobic CD cage. The formation of a water cluster to donate a proton to the imino group located inside the cavity controls the imine-protonation rate of $^{-}$OQN. Our study has shown that the molecular cages of CD can modulate the energetics and the solvent structural dynamics of polar reactions such as acid–base reactions.

Acknowledgments

This work was supported by the Korea Research Foundation Grant (KRF-2004-015-C00230). Y.S.L. also thanks the scholarship of the BK21 Program.

References

[1] O.F. Mohammed, D. Pines, J. Dreyer, E. Pines, E.T.J. Nibbering, Science 83 (2005) 310.
[2] D.E. Folmer, E.S. Wisniewski, J.R. Stairs, A.W. Castleman Jr., J. Phys. Chem. A 104 (2000) 10545.
[3] A. Douhal, F. Lahmani, A.H. Zewail, Chem. Phys. 207 (1996) 477.
[4] K.M. Solntsev, D. Huppert, N. Agmon, L.M. Tolbert, J. Phys. Chem. A 104 (2000) 4658.
[5] L.M. Tolbert, K.M. Solntsev, Acc. Chem. Res. 35 (2002) 19.
[6] O.-H. Kwon, Y.-S. Lee, H.J. Park, Y. Kim, D.-J. Jang, Angew. Chem. Int. Ed. 43 (2004) 5792.
[7] O.-H. Kwon, Y.-S. Lee, B.K. Yoo, D.-J. Jang, Angew. Chem. Int. Ed. 45 (2006) 415.
[8] M.E. Tuckerman, D. Marx, M.L. Klein, M. Parrinello, Science 275 (1997) 817.
[9] O.-H. Kwon, H. Doo, Y.-S. Lee, D.-J. Jang, ChemPhysChem 4 (2003) 1079.
[10] T.-G. Kim, Y. Kim, D.-J. Jang, J. Phys. Chem. A 105 (2001) 4328.
[11] S.-I. Lee, D.-J. Jang, J. Phys. Chem. 99 (1995) 7537.
[12] T.-G. Kim, S.-I. Lee, D.-J. Jang, Y. Kim, J. Phys. Chem. 99 (1995) 12698.
[13] S.F. Mason, J. Philip, B.E. Smith, J. Chem. Soc. A (1968) 3051.
[14] O. Poizat, E. Bardez, G. Buntinx, V. Alain, J. Phys. Chem. A 108 (2004) 1873.
[15] H. Yu, O.-H. Kwon, D.-J. Jang, J. Phys. Chem. A 108 (2004) 5932.
[16] K.M. Solntsev, C.E. Clower, L.M. Tolbert, D. Huppert, J. Am. Chem. Soc. 127 (2005) 8534.
[17] I. García-Ochoa, M.-A. Díez López, M.H. Viñas, L. Santos, E. Martínez Ataz, F. Sánchez, A. Douhal, Chem. Phys. Lett. 296 (1998) 335.
[18] H.J. Park, O.-H. Kwon, C.S. Ah, D.-J. Jang, J. Phys. Chem. B 109 (2005) 3938.
[19] A. Douhal, Acc. Chem. Res. 37 (2004) 349.
[20] R. Gepshtein, P. Leiderman, D. Huppert, E. Project, E. Nachliel, M. Gutman, J. Phys. Chem. B 110 (2006) 26354.
[21] A. Douhal, Chem. Rev. 104 (2004) 1955.
[22] O.H. Kwon, T.G. Kim, Y.-S. Lee, D.-J. Jang, J. Phys. Chem. B 110 (2006) 11997.
[23] K. Bhattacharyya, Acc. Chem. Res. 36 (2003) 95.
[24] O.H. Kwon, D.-J. Jang, J. Phys. Chem. B 109 (2005) 8049.
[25] O.H. Kwon, D.-J. Jang, J. Phys. Chem. B 109 (2005) 20479.
[26] Y.-S. Lee, H.J.D. Park, -J. Jang, Bull. Korean Chem. Soc. 27 (2006) 1450.
[27] R.G. Bate, Determination of pH, John Wiley & Sons, New York, 1973 (Chapter 11).
[28] A. Schäfer, H. Horn, R. Ahlrichs, J. Chem. Phys. 97 (1992) 2571.
[29] L. Tormo, J.A. Organero, A. Douhal, J. Phys. Chem. B 110 (2005) 17848.
[30] P.-T. Chou, W.-S. Yu, Y.-M. Cheng, S.-C. Pu, Y.-C. Yu, Y.-C. Lin, C.-H. Huang, C.-T. Chen, J. Phys. Chem. A 108 (2004) 6487.
[31] L. Giestas, C. Yihwa, J.C. Lima, C. Vautier-Giongo, A. Lopes, A.L. Maçanita, F.H. Quina, J. Phys. Chem. A 107 (2003) 3263.
[32] (a) E. Pines, D. Huppert, M. Gutman, N. Nachliel, M. Fishman, J. Phys. Chem. 90 (1986) 6366;
(b) E. Bardez, A. Chatelain, B. Larrey, B. Valeur, J. Phys. Chem. 98 (1994) 2357.
[33] E. Pines, D. Pines, T. Barak, B.-Z. Magnes, L.M. Tolbert, J.E. Haubrich, Berl. Bunsenges. Phys. Chem. 102 (1998) 511.
[34] E. Pines, B.-Z. Magnes, M.J. Lang, G.R. Fleming, Chem. Phys. Lett. 281 (1997) 413.
[35] B. Cohen, P. Leiderman, D. Huppert, J. Phys. Chem. A 106 (2002) 11115.
[36] S. Senapati, A. Chandra, J. Phys. Chem. B 105 (2001) 5106.